



ANALYSIS ON SHEAR FAILURE OF PHC PILES UNDER DIFFERENT LEVELS OF AXIAL LOAD RATIOS

Y. P. Oktiovan⁽¹⁾, T. Otaki⁽²⁾, T. Obara⁽³⁾, S. Kono⁽⁴⁾, Y. Asai⁽⁵⁾, K. Kobayashi⁽⁶⁾, H. Watanabe⁽⁷⁾, T. Mukai⁽⁷⁾,
D. Mukai⁽⁸⁾

⁽¹⁾ Graduate Student, Tokyo Institute of Technology, yopi1838@gmail.com

⁽²⁾ Daiwa House, Tokyo, Japan

⁽³⁾ Assistant Professor, Inst. of Innovative Research, Tokyo Inst. of Technology, Japan, obara.t.ac@m.titech.ac.jp

⁽⁴⁾ Professor, Inst. of Innovative Research, Tokyo Inst. of Technology, Japan, kono.s.ae@m.titech.ac.jp

⁽⁵⁾ Concrete Pile and Pole Industrial Technology Association, Tokyo, Japan

⁽⁶⁾ Fujita Corporation, Tokyo, Japan

⁽⁷⁾ Research Fellow, Building Research Institute, Japan, wata_h@kenken.go.jp, t_mukai@kenken.go.jp

⁽⁸⁾ Associate Professor, Univ. of Wyoming, dmukai@uwyo.edu

Abstract

Based on the earthquake damage reports from the 1995 Hyogoken-Nanbu and 2011 Great East Japan earthquakes, severe damages were observed in precast high strength concrete (PHC) piles in schools and commercial housings. These precast concrete piles were designed according to the 1981 Japanese seismic design standard for allowable stress design methods for small and medium-scale earthquakes. Therefore, the predicted design capacity for these PHC piles under large scale earthquakes was relatively unknown. This is particularly dangerous since the post-peak brittle behavior of PHC piles was also immediately followed by a rapid drop in the shear capacity of PHC piles. Numerous researchers have focused on confirming the shear capacity of PHC piles subjected to small and medium earthquake loads. However, there are few studies that focused on in-depth investigation of the shear damage of PHC piles when subjected to large earthquake loads. This research focuses on conducting a 3-D finite element analysis based on the data obtained from the shear experiments of three PHC piles subjected to large earthquake loads. The piles were tested under constant compression and tension axial loads (total axial load ratios of -0.04, 0.19, 0.32, where negative indicates tension axial load) as well as anti-symmetric cyclic lateral load.

The finite element analysis was conducted using FINAL, a non-linear finite element analysis program for concrete structures. A smeared approach was utilized when modelling the spiral reinforcement while a discrete modelling approach was used to model the prestressing bars in the finite element model. Fracture energy criteria as well as the tension softening mechanism were also considered when defining the constitutive model for concrete in order to allow a realistic simulation of crack propagation in PHC piles. The analysis results showed that the models were able to capture the experimental results of three PHC piles reasonably well in terms of global response (lateral load – drift ratio relationship) with an average ratio of analytical to experimental peak capacity at 0.96 and an average ratio of analytical to experimental corresponding peak drift ratio at 0.92. The local response comparison between the analytical and experimental results were in a good agreement in terms of crack patterns, as well as strain distributions of prestressing bars. The analytical model managed to reproduce cracks with orientations nearly parallel to the axis of piles, similar to those observed during experiments for the compressive axially loaded specimens. This research concludes that when PHC piles are subjected to relatively small axial load ratios, allowable stress design based on the principal stress of PHC pile is considered adequate while new design guidelines with regards to the shear capacity of PHC piles subjected to large axial load ratios are needed.

Keywords: Precast PHC pile; shear failure; non-linear finite element method; axial load ratio; shear span ratio



1. Introduction

The Design Guidelines for Foundations of Buildings Against Seismic Forces proposed by the Building Center of Japan [1] was implemented generally as the primary design for commercial housing and is based on allowable stress design. At the moment, this particular design method was considered adequate for seismic design of sub-structure systems. For precast piles such as prestressing high strength concrete (PHC) piles, prestressing reinforced concrete (PRC) piles as well as cast-in-place piles, seismic design for sub-structure systems was not legally required for commercial housing since human casualties caused by failures on sub-structure systems did not occur. This seismic design concept for precast piles persisted until the Architectural Institute of Japan (AIJ) published the new guidelines for soil and foundations in 2019.

Based on the 2011 Great East Japan earthquake damage report published by Kaneko *et. al.* [2] on buildings with precast concrete piles, severe damages were observed in precast concrete (PC) piles and PHC piles, shown in Fig. 1a and Fig. 1b, respectively. Kaneko *et. al.* [2] also stated that in the case of PHC piles, the damage on PHC piles with or without concrete filling material in the hollow section were similar. It was observed that a wide range of PHC piles suffered damage due to building settlements and inclinations. The PHC pile damage was divided into two types; piles that failed in shear and piles that failed due to the loss of performance of bearing capacity. These piles were designed according to the 1981 Japanese seismic design standard proposed by the Building Center of Japan [1] for sub-structure systems subjected to small- and medium-scale earthquakes. Therefore, the predicted design capacity for PHC piles under large-scale earthquake was outside the scope of this standard. This is particularly dangerous since the post-peak behaviour of PHC piles was not only followed by excessive spalling in the outer section of the piles, but also followed by the rapid drop of shear and bearing capacity of the PHC piles.

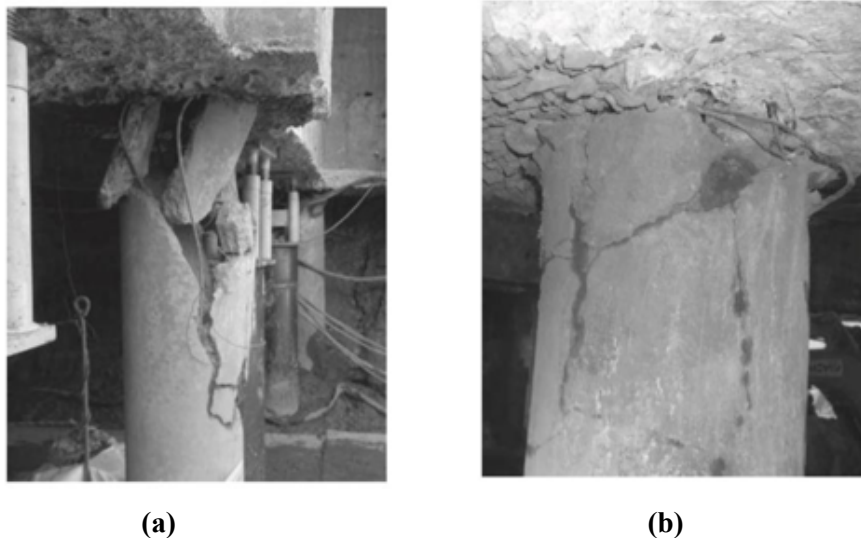


Fig. 1 – Damage observed at (a) PC pile and (b) PHC pile after 2011 Great East Japan Earthquake (Kaneko *et. al.* [2]).

Based on these findings, It is clear that the allowable stress design used for the seismic design of foundations members is inadequate for large-scale earthquakes. Efforts were then made evaluate and clarify the seismic performance of foundation members. The result of these efforts is the recently published draft of AIJ Guidelines for Seismic Design of Reinforced Concrete Foundation Members by the Architectural Institute of Japan [3], hereby termed as the 2017 AIJ Guidelines. The draft also provided structural performance evaluation methods for PRC and PHC piles subjected to severe earthquakes with regards to the flexural, shear, and bearing capacity of the system as well as the behaviour of pile structures when subjected to axial load. The 2017 AIJ Guidelines were used as the design basis for the three PHC piles tested in this research.



Previously, regarding the shear performance of PHC piles, numerous shear experiments were conducted to confirm the shear strength of precast PHC piles subjected to small to medium earthquake loads. Kokusho, *et. al.* [4] conducted experiment on 30 specimens of PHC piles in order to confirm the mechanical properties by changing several important parameters, such as the number of prestressing bars, spiral reinforcement ratio, effective prestressing, as well as applied axial load ratio. The researchers found that under high axial load, PHC piles did not experience any improvement in terms of deformation capability when other important parameters were altered.

In this research, three PHC piles were tested under constant tensile and high compressive axial loads as well as anti-symmetric cyclic lateral load in order to simulate the behavior of PHC piles when subjected to large earthquake load. The experiment attempted to confirm the ultimate shear behavior of PHC piles tested under constant axial load. Finite element analysis (FEA) was then conducted based on the experimental results to simulate the experimental results in terms of lateral load-drift ratio relationship for the global response crack propagation, strains in prestressing bars, as well as the stress distribution for the local response.

2. Experimental Program

2.1 Specimens and materials

In order to observe the ultimate condition of PHC piles under large earthquakes, anti-symmetric cyclic loading tests were conducted on three PHC piles. The piles were tested horizontally as a simply supported system, presented in Fig. 2. Pile specifications and the mechanical properties of concrete, prestressing bars and spiral reinforcement are shown in Table 1 and Table 2, respectively.

The outer diameter of the pile specimens was set at 400 mm with concrete thickness of 75 mm. All PHC pile specimens were designed as PHC pile type-C under specifications provided in JIS A 5363 [5]. PHC pile type-C was designed with effective prestressing force of roughly 10 MPa with 10-11.2mm prestressing bars. The yield strain at 0.2% offset was 8021 μ . These prestressing bars were held in place by 3.2 mm spiral reinforcement spaced every 100 mm. The yield strain of the spiral reinforcement at 0.2% strain was 4263 μ .

The pile specimens were manufactured using centrifugal concrete casting and autoclave curing. The concrete Young's moduli shown in Table 2 were taken as the slope of a straight line connecting the origin to the point where concrete stress is $1/3f'_c$. The concrete design strength was set at 105 MPa. The concrete material was tested under specifications provided in JIS A 1136 [6] with specimen dimension as follows: outer diameter 200 mm, height 300 mm, and thickness 40 mm. Tensile splitting tests were conducted using test cylinders with dimension of $\phi 100 \times 200$ mm. All concrete material tests were conducted at the same time of the experiment. Stress and strain relationship obtained from material test for concrete and prestressing bars will be compared with the material constitutive model in Section 4.1.

2.2 Test method and measurement

Fig. 3 shows the diagram of the loading setup of the PHC pile experiment. The total span of the pile specimen was 8000 mm with anti-symmetric cyclic load applied at a 1000 mm span in the middle of the pile specimen. The piles were tested according to the standard provided in JIS A 5363 [5], hence there was no soil-structure interaction considered in the experiment.

In this experiment, the pile specimens were tested using a simply supported system where piles were situated horizontally with support points located at both ends of the pile. These support points were prestressing using 4 32-mm diameter prestressing bars. Two frame-lifting jacks were placed at both ends of the pile specimen in order to offset the self-weight of the pile specimen and the experiment frame. Axial load was applied using 4 jacks each with a capacity of 5 MN in compression and 2 MN in tension.



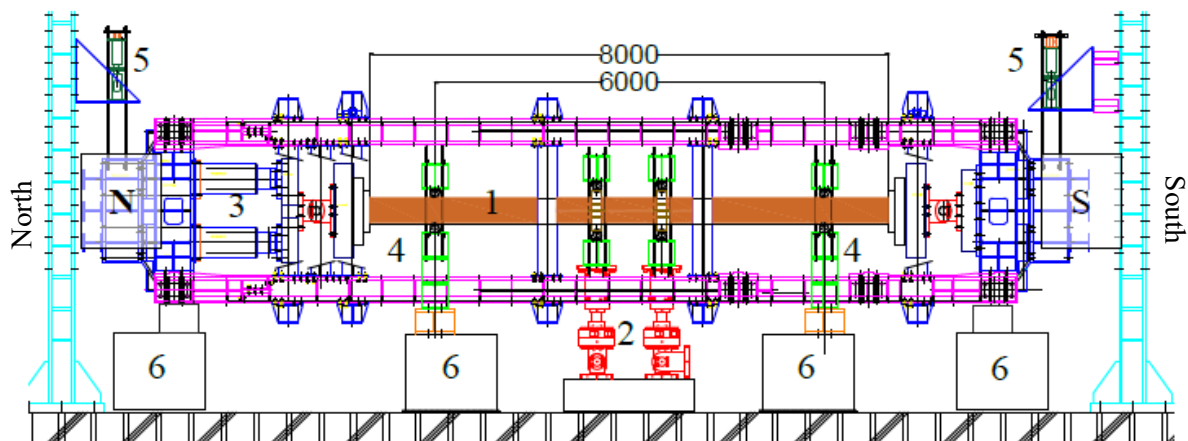
Table 1 – Mechanical properties of concrete, prestressing bars, and spiral reinforcement

Properties		Description	PHC18	PHC19	PHC20
Concrete	f_c (MPa)	Compressive strength	114	117	116
	ϵ_c (μ)	Compressive strain	2304	2403	2323
	f_t (MPa)	Tensile splitting strength	5.1	5.5	6.2
	E_c (MPa)	Young's modulus	49.1	48.7	50.4

Table 2 – Pile specimen cross section and axial load details

Pile	Outer diameter	Concrete thickness	Applied Axial Load	Effective Prestressing	Axial Load Capacity	Axial Load Ratio
	D	t_c	N	N_e	N_{max}	$\frac{N + N_e}{N_{max}}$
	mm	mm	kN	kN	kN	
PHC18	400	76.1	-344	789	10037	-0.04
PHC19	400	77.3	1368	794	10375	0.19
PHC20	400	75.5	2752	786	10131	0.32

While constant axial load was applied, anti-symmetric displacement-controlled cyclic load was applied at the midspan of the pile specimen using two lateral jacks situated 1000 mm apart. The two lateral loading jacks were situated at the bottom of the pile specimen, as shown in Fig 3, each with a capacity of 4 MN in compression and 1.5 MN in tension. The load was then transferred from lateral loading jacks to loading bands attached to the pile specimens. The loading jacks and loading bands were connected to the floor through support blocks which was prestressed using 4 32-mm diameter prestressing bars.



1. Pile specimen, 2. lateral loading jacks, 3. Axial loading jacks, 4. Specimen support points, 5. Frame lifting jacks, 6. Concrete blocks

Fig. 2 – Pile experiment loading setup



The prestressing bars on the loading bands allow pulling motion of the pile specimens when the lateral loading jack was retracted. Both loading bands and support points were not directly attached to the pile specimen, allowing sliding of the pile specimen in the axial direction. To measure the longitudinal strain in the prestressing bars and spiral reinforcement, strain gauges were attached on top and bottom prestressing bars as well as the center section of the spiral reinforcement. The strain gauges were attached only in the mid-span of the pile specimen, as shown in Fig. 3. P1, P5, P6 and P10 were placed 100 mm from the center of the loading bands. The longitudinal strain distribution will be shown in Section 4.3 along with the analysis results,.

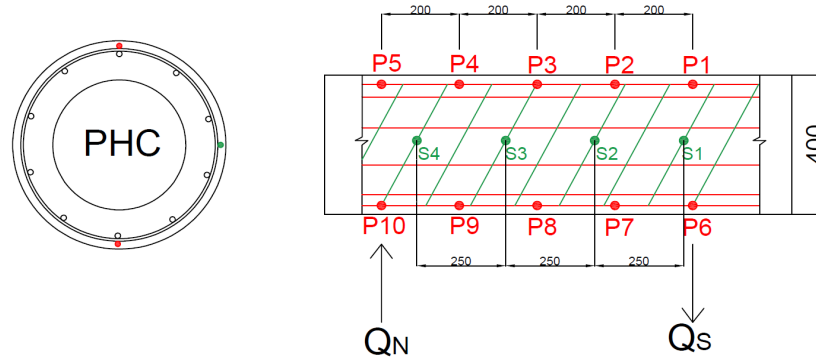


Fig.3 – Strain gauges arrangement at the center of PHC pile specimen

Deformations of the pile specimens were measured using horizontal displacement gauges, as shown in Fig. 4. The displacement gauges were used to calculate the drift ratio in this experiment. The drift ratio was taken from displacement gauges located 175 mm away from both loading bands since attaching displacement gauges directly to the loading bands was impossible.

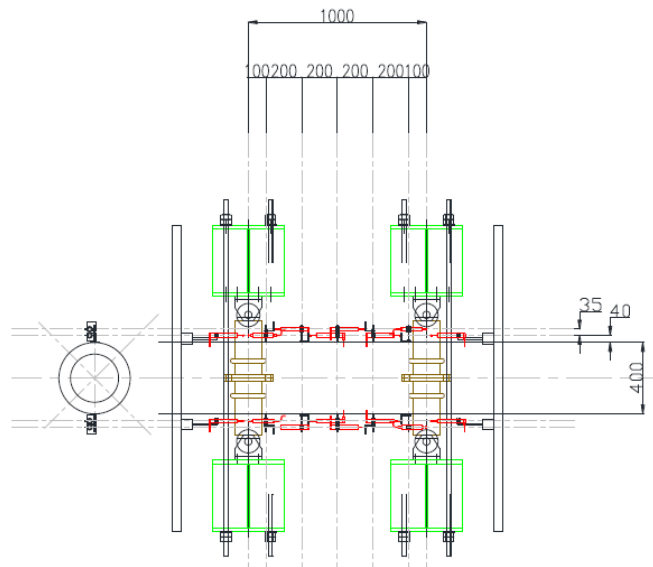


Fig.4 – Displacement gauges arrangement at the mid-span of PHC pile specimen

Displacement gauge on the left was used to measure the displacement on the left loading band, δ_{+175} , while displacement gauge on the right was used to measure displacement on the right loading band, δ_{-175} . Moment diagram of the pile specimen is shown in Fig. 5. Based on this moment diagram, the member drift ratio R can be calculated using Eq. 1:

$$R = \frac{\delta_{+175} - \delta_{-175}}{L + 350} \tag{1}$$

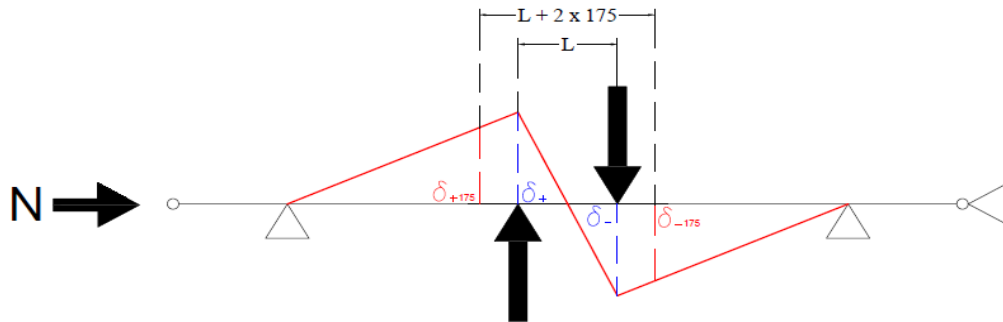


Fig.5 – Moment diagram of PHC pile specimen.

On the other hand, the lateral load, Q , as well as the axial load, N , values were measured by the corresponding load cells on each loading jacks. The cyclic loads were applied with incremental drift ratio, R , of 0.125%, 0.25%, 0.5%, 0.75%, and 1.0%. Each drift ratio was applied twice. If the specimen experienced excessive spalling and the shear capacity of the pile decreased up to 20% of the maximum capacity, the pile loading sequence was advanced to a member drift angle of $R = 1.0\%$. Experimental results in terms of lateral load – drift ratio relationship, crack pattern, and longitudinal strain distribution will be shown along with the results from the finite element analysis in Section 4.

3. Finite Element Modeling

In order to evaluate damage occurring during the experiment as well as the failure mechanism of PHC pile when subjected to high axial load ratios, three finite element models were created, based on the experimental results explained in the previous section, using the commercial finite element analysis platform FINAL [7]. Cyclic analysis was carried out under displacement control anti-symmetric lateral load and constant axial load. Both global and local responses of the pile system were compared to the experimental results.

Numerical analysis of high strength concrete members cannot be addressed solely by the concrete compressive strength since the crack surfaces in high strength concrete are characterized by smoother fracture plane compared to those on normal strength concrete. Moreover, high strength concrete damage is normally characterized by sudden stress release after peak capacity is reached. Therefore, aside from compressive and tensile concrete constitutive models, concrete failure criteria and fracture mechanics should also be defined in order to provide better prediction of the behavior of PHC pile.

3.1 Element definition

Hexahedral elements defined as 8-node iso-parametric element with 8 integration points were utilized for concrete elements as well as the auxiliary elements such as loading bands and end plates. The hexahedral elements in the auxiliary elements were defined as rigid elements in order to avoid stress concentration on the auxiliary elements. The nodes in the hexahedral elements were defined in polar coordinates. The mesh aspect ratio of PHC pile center was set at 1.33 while the mesh aspect ratio of regions close to the loading bands was set at 1.05.

There were two methods utilized when building the finite element model for steel elements of PHC pile such as prestressing bars and spiral reinforcement. The spiral reinforcement was embedded inside the corresponding concrete elements. This particular method is defined as a smeared approach. The prestressing bars were modelled as truss elements where the only active degree of freedom was translation in the axial direction. The nodes on prestressing bars and nodes at the corresponding concrete elements were shared through zero length interface elements. This method is defined as a discrete modelling approach.

3.2 Material constitutive models

The material model utilized in the finite element model is the proprietary constitutive model used in FINAL [7]. Concrete compressive strength, tensile splitting strength, and concrete Young's modulus, obtained from



material tests shown in Table 2, were utilized as inputs to the concrete material constitutive model. The compressive constitutive model by Fafitis and Shah [8] for high-strength concrete was based on several sets of experimental data on confined and unconfined high strength concrete members. Concrete failure criteria for the finite element model was based on the work of Ottosen [9] with experimentally derived governing parameters. The tension softening model defined by Izumo, *et. al.* [10] was utilized as the concrete tensile constitutive model. The equation to determine the tensile strength is provided in Eq. 2:

$$\frac{\sigma_t}{f_t} = \left(\frac{\varepsilon_{cr}}{\varepsilon_t} \right)^c \quad (2)$$

Where σ_t is the average tensile stress in MPa, f_t is the tensile splitting stress in MPa, ε_{cr} is the tensile cracking strain, ε_t is the average tensile strain and c is the tension softening parameter. The c parameter was used to reflect the energy release mechanism of either lightly or heavily reinforced concrete. On the other hand, A modified Menegotto-Pinto model proposed by Filippou, *et. al.* [11] was utilized as the steel constitutive model for prestressing bars and spiral reinforcement in the finite element model.

3.3 Boundary conditions

The typical mesh of the finite element model is shown in Fig. 6 along with the boundary conditions. The anti-symmetric loads (denoted as Q_L and Q_R , where L and R denote left and right side of the model) were applied to the bottommost loading band nodes. The load was then transferred to the pile concrete elements through connector elements. The connector element was designed as a frictionless contact surface in order to allow sliding in the axial direction. Constraint in the lateral direction was applied to nodes located 2500mm away from center of both left and right side of the loading bands which coincides with the support points in the experimental setup, shown in Fig. 3. Due to symmetry of the PHC pile cross section, only half of the pile specimen was modelled in this analytical model.

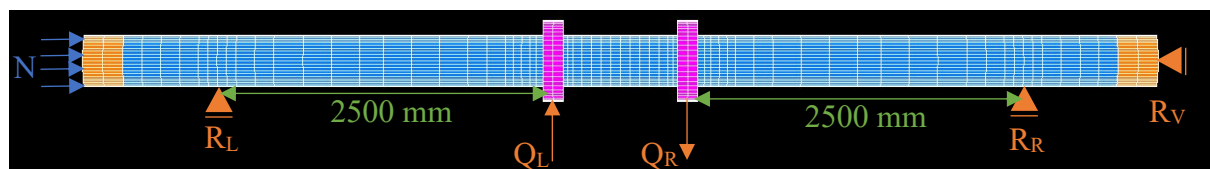


Fig.6 – Typical finite element model of PHC pile.

4. Analysis Results

The analytical results compared in this research includes the single element material test, lateral load – drift ratio relationship, crack pattern comparison, as well as longitudinal strain distributions on prestressing bars.

4.1 Single element test

The material constitutive model defined in Section 3.2 needs to be confirmed with the results obtained from material test during experiment. A single brick element was used for the uniaxial material test on the finite element program. The configurations of both concrete element and steel elements are shown in Fig. 8 along with the boundary conditions. The boundary condition was set so that each directions of the brick element were restrained.

Fig. 9 shows the result of the single element material test for PHC19 finite element model as well as its comparison to the experimental test result. Since the high strength concrete cylinder explodes immediately after peak load was reached, the post-peak behavior for concrete compressive test could not be properly compared. It can be seen that the material constitutive models captured the stress-strain behavior of each corresponding materials relatively well.

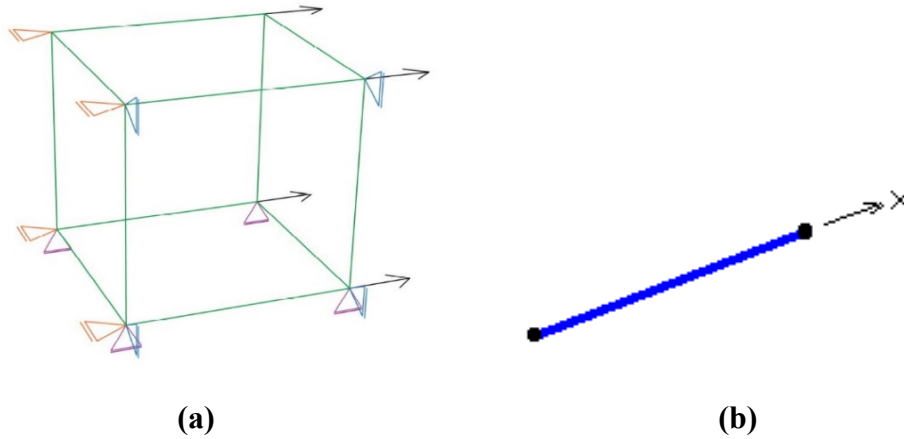


Fig.8 – Material test configuration for (a) concrete brick element and (b) prestressing bars and spiral reinforcement line elements

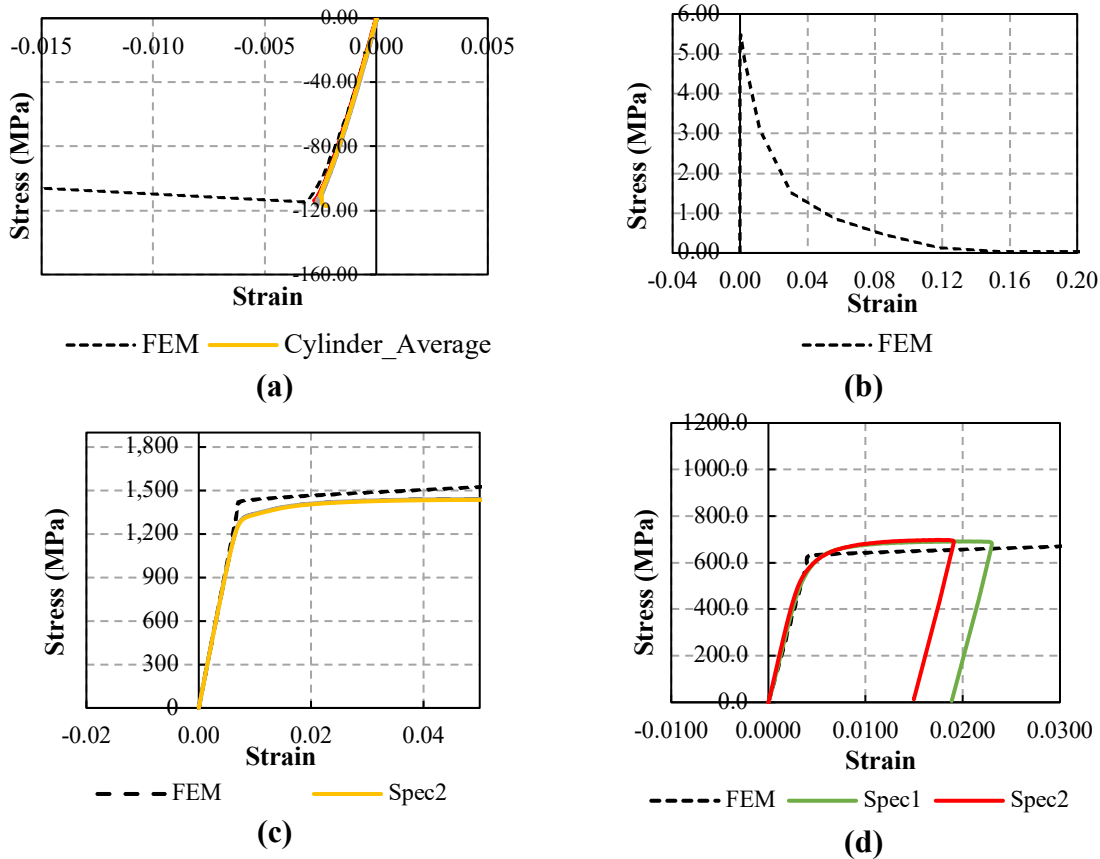


Fig.9 – Stress strain relationship of (a) concrete in compression, (b) concrete in tension, (c) prestressing bars and (d) spiral reinforcement



4.2 Lateral load – drift ratio (Q – R) relationship

The global response of the pile model is represented by the lateral load – drift ratio relationship (hereby termed the Q – R relationship). Fig. 10 shows the Q-R relationship of all three pile models along with the comparison to the experimental results, shown in the dotted line. The important events observed during loading are shown in Fig. 10 as well. Shear crack (denoted as SC) is defined as the point where cracks with orientation of approximately 45° occurred along the pile center. Peak point (denoted as Peak) is defined as the point where the pile reached its maximum capacity. In this experiment, ultimate point (denoted as Ult) is defined as the point where pile shear capacity dropped 20% from the maximum capacity.

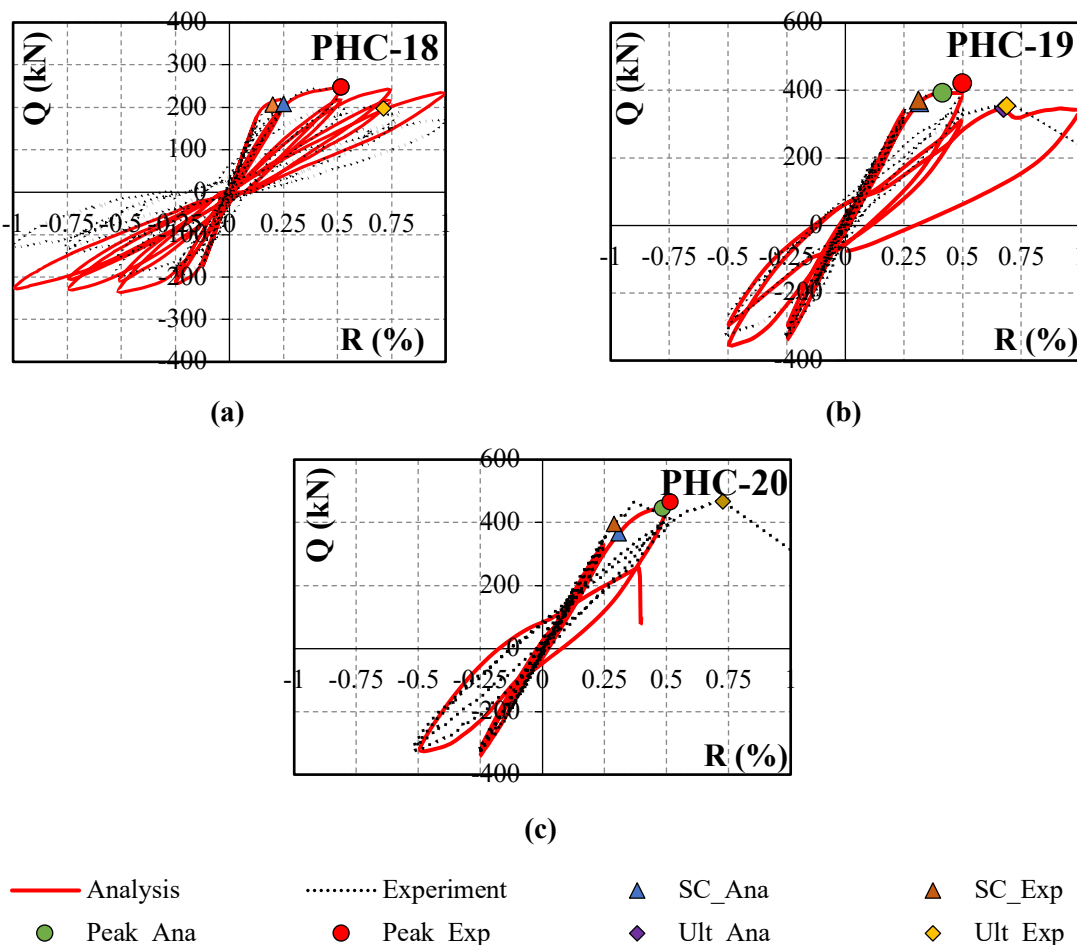


Fig.10 – Lateral load – drift ratio relationship of all PHC pile models

As shown in Fig. 10, the analytical model managed to simulate the experimental results with relatively good accuracy. The important events were predicted with an average Q_{FEM}/Q_{EXP} (ratio of analytically predicted to experimentally observed capacity) of 0.96 and an average R_{FEM}/R_{EXP} of 0.92. Fig.10a shows that the Q-R response of the analytical model for PHC18 after peak capacity was reached was relatively different than the experimental results where capacity drop after peak for the analytical model was found to be slower than that observed in the experimental results.

On the other hand, the post-peak behavior of PHC19 and PHC20, shown in Fig. 10b and 10c respectively, were accurately predicted by the finite element model. The PHC19 model was able to reach the ultimate point similar to the experimental results while the PHC20 model diverged before reaching the ultimate point observed during experiment. Based on the Q-R relationship comparison, it can be seen that the FEM model accurately captured the global response of the PHC pile experiment.

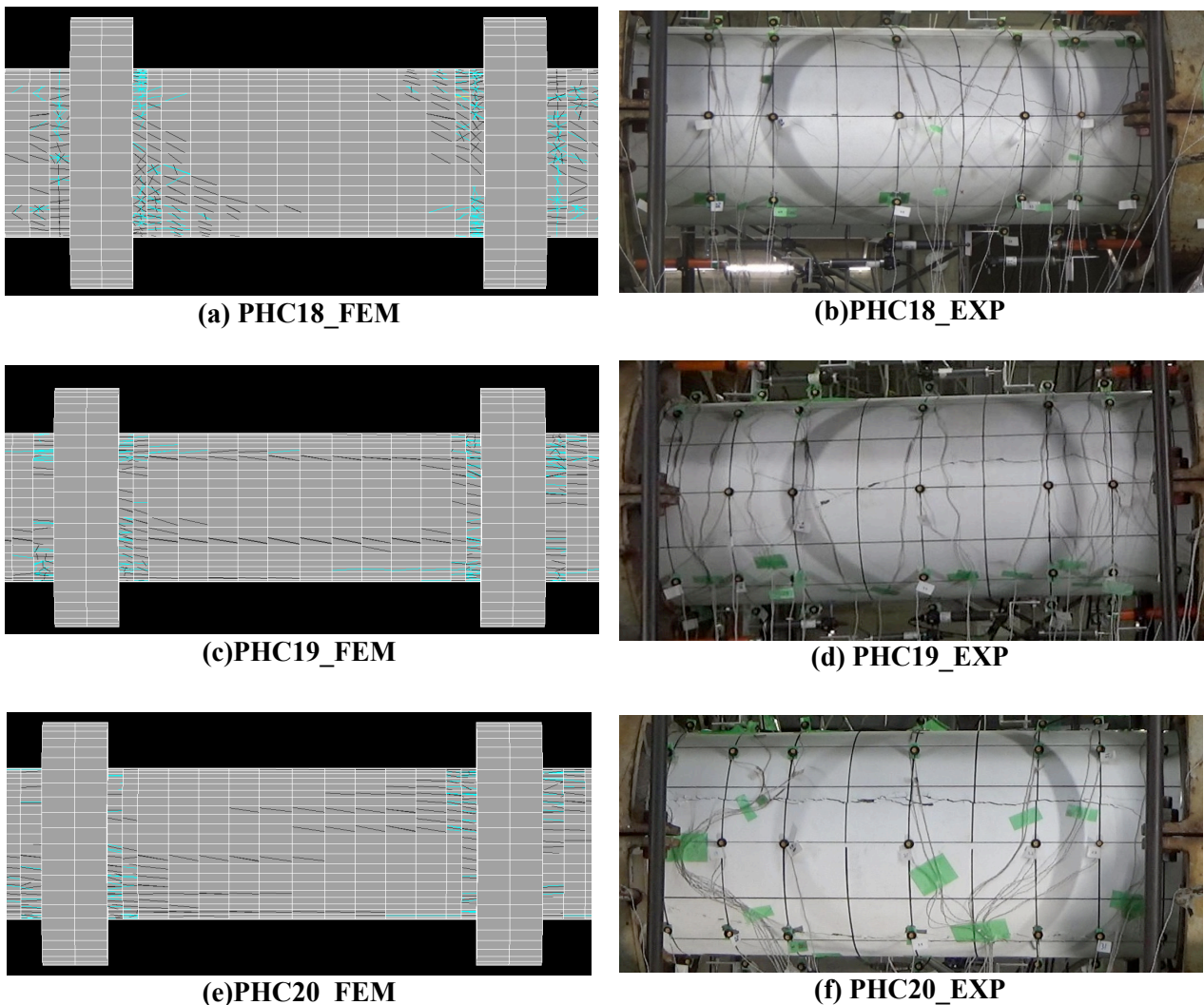


Fig.11 – Crack pattern observed at peak load during analysis and experiment

4.2 Crack pattern

The analytically predicted crack patterns at peak point in the positive loading cycle of all three pile models are shown in Fig 11 along with the corresponding experimental results. Blue lines indicate closed cracks while black lines indicate open cracks during the recorded cycle. The crack pattern of PHC18 at peak point shown in Fig. 11a shows diagonal shear cracks propagating from compressing points of the loading bands with no occurrence of crack patterns parallel to the axial loading direction, which is similar to patterns found during the experiment presented in Fig. 11b. This could be caused by the strut mechanism which was the dominant mechanism in PHC18. The crack pattern in both the experiment and analysis were propagating diagonally forming a compression strut from the compressing points of one loading band to the other, indicating the strut mechanism.

In the crack pattern at peak point of PHC19 shown in Fig. 11c, the cracks parallel to the axial direction also occurred in the analytically predicted crack pattern with transition diagonal shear cracks found at the concrete elements relatively close to the loading bands, similar to those observed during the experiment shown in Fig. 11d. Finally, the crack pattern of PHC20 shown in Fig. 11e is extremely horizontal with no occurrence of diagonal shear cracks, which is similar to the condition observed during the experiment presented in Fig. 11f. Comparing these three piles, it can be seen that there is a shift in load carrying mechanism parallel to longitudinal axis as the total axial load ratio is increased for PHC piles.



4.3 Strain distribution in prestressing bars

The strain distribution comparison between analysis and experiment for both top and bottom sections of the pile center is presented in Fig. 12. Lines of the same color in these plots are at the same position in the axial loading direction (i.e. P5 and P10, P4 and P9 and so on, as shown in Fig. 4). The analytically predicted strain in the prestressing bars is obtained from the axial direction strain of the prestressing bar line elements at the same location to those in the experiments.

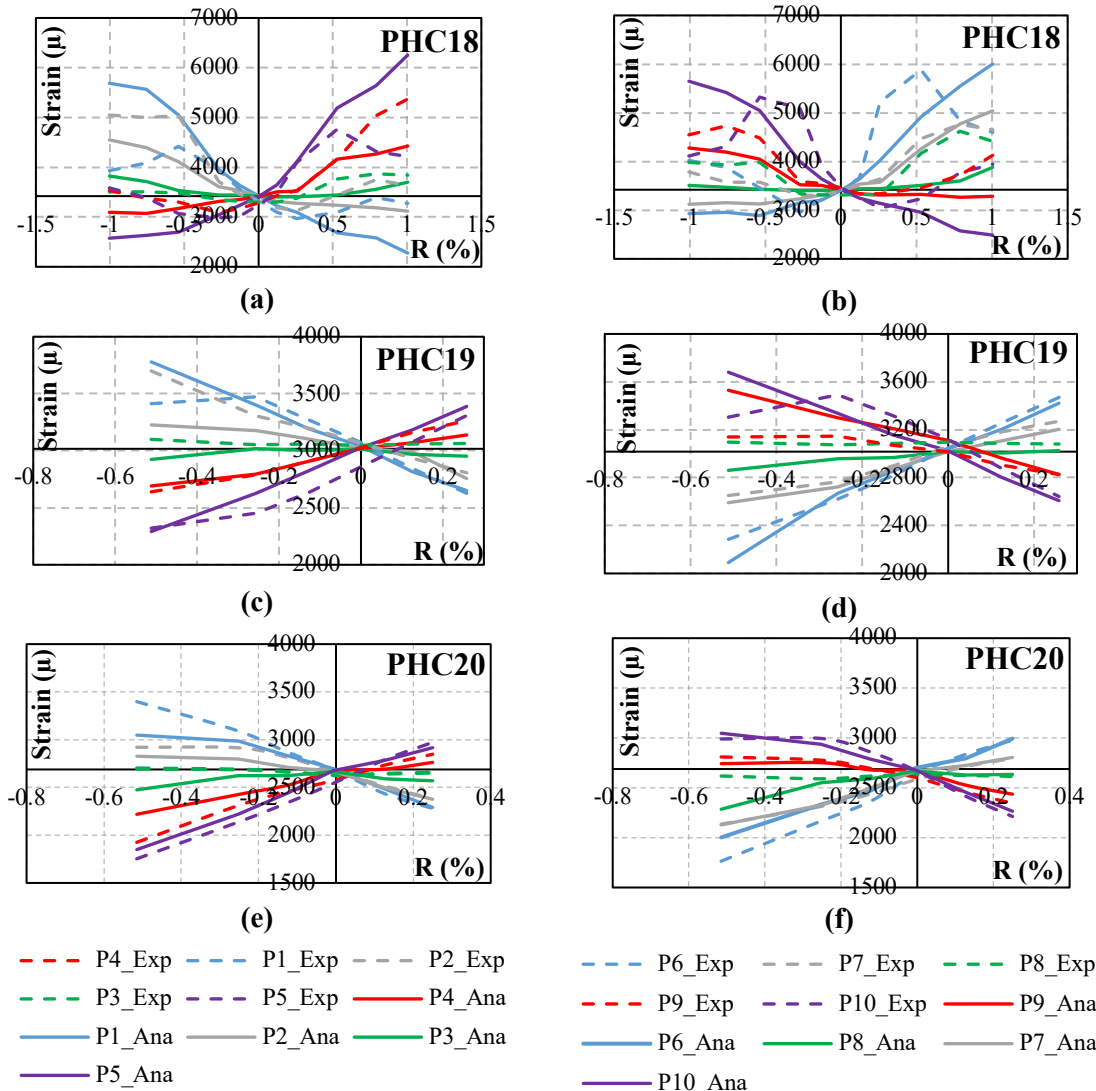


Fig.12 – Strain distribution of prestressing bars at top and bottom section of PHC pile from analysis and experiment

The longitudinal strain at prestressing bars of PHC18 obtained from finite element analysis was in a good agreement with the experimental results up to a member drift angle of $R = 0.5\%$ where both analysis and experiment have reached their maximum capacity. However, due to relatively small drop in post-peak capacity found in the analytical model of PHC18, the post-peak strain distribution of PHC18 pile model became relatively different to those observed during experiments.

On the other hand, the analytically predicted strain of prestressing bars on PHC19 and PHC20 were captured significantly well by the models on both top and bottom prestressing bars. PHC19 and PHC20 analytical models managed to predict strain in prestressing bars with 10% and 15% maximum error, respectively. Both experiment and analytical model did not reach the yield strain of prestressing bars.



5. Conclusions

The conclusions of this research are as follows:

- The finite element models of three tested PHC piles were able to predict the global response in terms of Q – R relationship of the pile reasonably well with an average Q_{FEM}/Q_{EXP} (ratio of analytically predicted to experimentally observed capacity) of 0.96 and an average R_{FEM}/R_{EXP} of 0.92.
- Local responses, represented by crack patterns and prestressing bars longitudinal strain distribution shown in Section 4, was nicely captured as well with crack orientations relatively close to 0° against the axial loading direction that propagated horizontally.
- Based on the crack pattern comparison, there seems to be a shift in load carrying mechanisms of PHC pile as the applied axial load ratio is increased. Parametric study should be conducted in order to observe at which axial load level did the PHC pile behavior started to change.

7. Acknowledgement

This work was supported financially by JSPS through two Grant-in-Aid programs (PI: Shuji Tamura and Susumu Kono). We are thankful to the Concrete Pile and Pole Industrial Technology Association and Steel encased Cast-in-place Concrete Piles Association for their expert advice and support. We are also thankful to the Consortium for Socio-Functional Continuity Technology (PI: S. Yamada), the Collaborative Research Project (Materials and Structures Laboratory), and the World Research Hub Initiative (Institute of Innovative Research), at Tokyo Institute of Technology for their generous support of this work.

8. References

- [1] Building Center of Japan, (1984): *Design guidelines for foundations of buildings against seismic forces*. Building Center of Japan (in Japanese)
- [2] Kaneko, O., et. al., (2012): Situations and analysis of damage to pile foundations of buildings in 2011 Great East Japan Earthquake. *Journal of Geotechnical Engineering: Soil and Foundation*, the Japanese Geotechnical Society (in Japanese)
- [3] AIJ, (2017): *AIJ Guidelines for Seismic Design of Reinforced Concrete Foundation Members (draft)*. Architectural Institute of Japan (in Japanese)
- [4] Kokusho, S., et. al. (1987): Experiments on The Seismic Behavior of PHC Piles.”, *Proceedings of Architectural Institute of Japan*, (in Japanese)
- [5] Japan Industrial Standard, (2016): Precast Concrete Products – General Rules for Methods of Performance Test. *JIS A 5363*, Japanese Standards Association (JSA) (in Japanese)
- [6] Japan Industrial Standard, (1993): Method of Test for Compressive Strength of Spun Concrete. *JIS G 1136*, Japanese Standards Association (JSA) (in Japanese)
- [7] ITOCHU Techno-solutions Corporations, (2015): *FINAL: 3-D Non-linear Analysis for Concrete Structures Manual*. Engineering Eye, Japan (in Japanese)
- [8] Fafitis, A. and Shah, S.P., (1985): Lateral Reinforcement for High-strength Concrete Columns. *ACI Special Publications*, No. SP – 87, pp. 213 – 232
- [9] Ottosen, N.S., (1977): A Failure Criterion for Concrete. *Journal of the Engineering Mechanics Division*, ASCE, Vol. 103, No. EM4, pp. 527 – 535
- [10] Izumo, J., Shima, H., and Okamura, H., (1989): Analytical Model of Reinforced Concrete Plate Element Subjected To In-plane Forces. *Journal of Japan Concrete Institute*, Vol. 25, No.9, pp. 107 – 120
- [11] Filippou, F.P., Popov, E.P., and Bertero, V.V., (1983): Effects of Bond Deterioration on Hysteretic Behavior of Reinforced Concrete Joints. *Research Report*, Earthquake Engineering Research Center, California, USA